stress because of global climate change. By the end of the century, however, the seasonal growing temperature is likely to exceed the hottest season on record in temperate countries (e.g., equivalent to what France experienced in 2003), and the future for agriculture in these regions will become equally daunting.

Second, the projected seasonal average temperature represents the median, not the tail, of the climate distribution and should therefore be considered the norm for the future. Indeed, the probability exceeds 90% that by the end of the century, the summer average temperature will exceed the hottest summer on record throughout the tropics and subtropics (Fig. 3B). Because these regions are home to about half the world's population, the human consequences of global climate change could be enormous.

Lastly, with growing season temperatures in excess of the hottest years on record for many countries, the stress on crops and livestock will become global in character. It will be extremely difficult to balance food deficits in one part of the world with food surpluses in another, unless major adaptation investments are made soon to develop crop varieties that are tolerant to heat and heat-induced water stress and irrigation systems suitable for diverse agroecosystems. The genetics, genomics, breeding, management, and engineering capacity for such adaptation can be developed globally but will be costly and will require political prioritization (*5*, *8*, *9*, *20*). National and international agricultural investments have been waning in recent decades and remain insufficient to meet near-term food needs in the world's poorest countries, to say nothing of longer-term needs in the face of climate change (*1*). History provides some guide to the magnitude and effects of high seasonal averaged temperature projected for the future. Ignoring climate projections at this stage will only result in the worst form of triage.

References and Notes

1. R. Naylor, W. Falcon, *Boston Rev.* **33**, 13 (2008).
2. We approximated the main growing season to be summer in the extratropics. Hence north of the equator we used the three-month average temperature June through August (and for south of the equator we used December through February), periods that broadly capture growing season conditions for many crops.
3. IPCC, *Fourth Assessment Report: Synthesis*, published online 17 November 2007, www.ipcc.ch/ipccreports/ar4-syr.htm.
4. World Bank, *World Development Report 2008: Agriculture for Development* (World Bank, Washington, DC, 2007).
5. W. Easterling *et al.*, in *Climate Change 2007: Impacts, Adaptation, and Vulnerability*, M. Parry *et al.*, Eds. (Cambridge Univ. Press, New York, 2007), p. 976.
6. D. Lobell, M. Burke, *Environ. Res. Lett.* **3**, 034007 (2008).
7. S. Peng *et al.*, *Proc. Natl. Acad. Sci. U.S.A.* **101**, 9971 (2004).
8. D. B. Lobell *et al.*, *Science* **319**, 607 (2008).
9. B. Barnabas *et al.*, *Plant Cell Environ.* **31**, 11 (2008).
10. W. Schlenker, M. J. Roberts, *Rev. Agric. Econ.* **28**, 391 (2006).
11. J. Larsen, *Earth Policy Institute*, published online 28 July 2006 (www.earth-policy.org/Updates/2006/Update56.htm).
12. P. Pirard *et al.*, *Eurosurveillance* **10**, 554 (2005).
13. A. De Bono *et al.*, "Environmental alert bulletin: Impacts of summer 2003 heat wave in Europe" (United Nations Environmental Programme, Nairobi, Kenya, 2004).
14. International Financial Statistics Database, "United States Gulf ports wheat prices," published online July 2008, www.imfstatistics.org.
15. D. Hathaway *et al.*, *Brookings Pap. Econ. Act.* **1**, 63 (1974).
16. N. Dronin, E. Bellinger, *Climate Dependence and Food Problems in Russia 1900-1990* (Central European Univ. Press, New York, 2005).
17. World Bank, *Africa Development Indicators 2007* (World Bank, Washington, DC, 2007).
18. S. Kandji, L. Verchot, J. Mackensen, *Climate Change and Variability in the Sahel Region: Impacts and Adaptation Strategies in the Agricultural Sector* (United Nations Environmental Programme and World Agroforestry Center, Nairobi, Kenya, 2006).
19. T. Jayne, in *The Transformation of Agri-Food Systems: Globalization, Supply Chains, and Smallholder Farmers*, E. B. McCullough *et al.*, Eds. (Earthscan, London, 2008).
20. S. Takeda, M. Matsuoka, *Nat. Rev. Genet.* **9**, 444 (2008).
21. To calculate the projected climate for 2090, we first added the observed temperature departures (in blue) to the change in the summer temperature, taken to be the mean summer temperature for 2080–2100 minus that for 1980–2000, simulated by each of the 23 climate models from the IPCC AR4 forced by the "middle of the road" emission scenario, A1B. We then combined the 23 × 107 projections to create the probability distribution function for summer temperature in 2090 (see SOM).
22. The probability distribution of future summer temperature is calculated as described in (*21*). Here, summer is defined north of the equator as the average temperature from June through August and south of the equator as December through February. In the immediate vicinity of the equator, values in Fig. 3 are qualitatively insensitive to the choice of months that define the season.

23. This work was made possible by grants from the NSF (grant SES 0433679) and the Tamaki Foundation. We thank M. Baker, M. Burke, W. Falcon, D. Kennedy, S.-H. Kim, D. Lobell, R. Nicholas, K. Niemer Johnson, K. Rennert, and D. Vimont for comments and/or assistance on the draft.

Supporting Online Material

www.sciencemag.org/cgi/content/full/323/5911/240/DC1
Materials and Methods
SOM Text
References and Notes

7 August 2008; accepted 2 December 2008
10.1126/science.1164363

Foraminiferal Isotope Evidence of Reduced Nitrogen Fixation in the Ice Age Atlantic Ocean

H. Ren,[1]* D. M. Sigman,[1] A. N. Meckler,[2] B. Plessen,[3] R. S. Robinson,[4] Y. Rosenthal,[5] G. H. Haug[6,7]

Fixed nitrogen (N) is a limiting nutrient for algae in the low-latitude ocean, and its oceanic inventory may have been higher during ice ages, thus helping to lower atmospheric CO_2 during those intervals. In organic matter within planktonic foraminifera shells in Caribbean Sea sediments, we found that the $^{15}N/^{14}N$ ratio from the last ice age is higher than that from the current interglacial, indicating a higher nitrate $^{15}N/^{14}N$ ratio in the Caribbean thermocline. This change and other species-specific differences are best explained by less N fixation in the Atlantic during the last ice age. The fixation decrease was most likely a response to a known ice age reduction in ocean N loss, and it would have worked to balance the ocean N budget and to curb ice age–interglacial change in the N inventory.

The sources of fixed N to the ocean are terrestrial runoff, atmospheric deposition, and, most important, marine N fixation. The main sinks are sedimentary denitrification, mostly in continental shelf sediments, and water column denitrification in the eastern tropical Pacific and the Arabian Sea. Sediment records from modern denitrification zones show clear N isotopic evidence of reduced water column denitrification during the Last Glacial Maximum (LGM) relative to the current interglacial (Holocene) (*1*, *2*). The history of other processes, especially N fixation, has proven more difficult to reconstruct. Decreased denitrification and/or increased N fixation would have raised the N inventory of the ocean during the LGM, thereby strengthening the ocean's biological pump and contributing to the observed reduction in atmospheric CO_2 during the ice age (*1*–*5*).

N fixation produces oceanic fixed N with $\delta^{15}N$ values between –2 and 0 per mil (‰), close to that of atmospheric N_2 (*6*, *7*). Sedimentary denitrification removes nitrate (NO_3^-) from the ocean with minimal isotope discrimination (*8*). In contrast, water column denitrification leaves residual nitrate enriched in ^{15}N that raises the $\delta^{15}N$ of mean ocean nitrate above that of newly

[1]Department of Geosciences, Guyot Hall, Princeton University, Princeton, NJ 08544, USA. [2]Geological and Planetary Sciences Division, California Institute of Technology, Pasadena, CA 91125, USA. [3]Helmholtz-Zentrum Potsdam, Deutsches GeoForschungsZentrum (GFZ), Potsdam 14473, Germany. [4]Graduate School of Oceanography, University of Rhode Island, Narragansett, RI 02882, USA. [5]Institute of Marine and Coastal Sciences and Department of Geological Sciences, Rutgers University, New Brunswick, NJ 08901, USA. [6]Geological Institute, Department of Earth Sciences, ETH Zürich, Zürich 8092, Switzerland. [7]DFG Leibniz Center for Earth Surface Process and Climate Studies, Institute for Geosciences, Potsdam University, Potsdam D-14476, Germany.

*To whom correspondence should be addressed. E-mail: hren@princeton.edu

fixed N (*9*). In the context of mean ocean nitrate with a $\delta^{15}N$ of ~5‰, N fixation causes a regional decrease in the $\delta^{15}N$ of thermocline nitrate, which is observed throughout the western subtropical and tropical North Atlantic (*10*–*12*). Thus, the $\delta^{15}N$ of organic N sinking out of the surface ocean, if preserved in the sediments, should record N fixation by two related mechanisms. First, most newly fixed N is remineralized in the thermocline, producing low-$\delta^{15}N$ nitrate, which is then provided repeatedly to the euphotic zone. Second, N fixation can contribute low-$\delta^{15}N$ N directly to the plankton in the surface ocean and the sinking flux that they produce. However, in the low-productivity, low-latitude

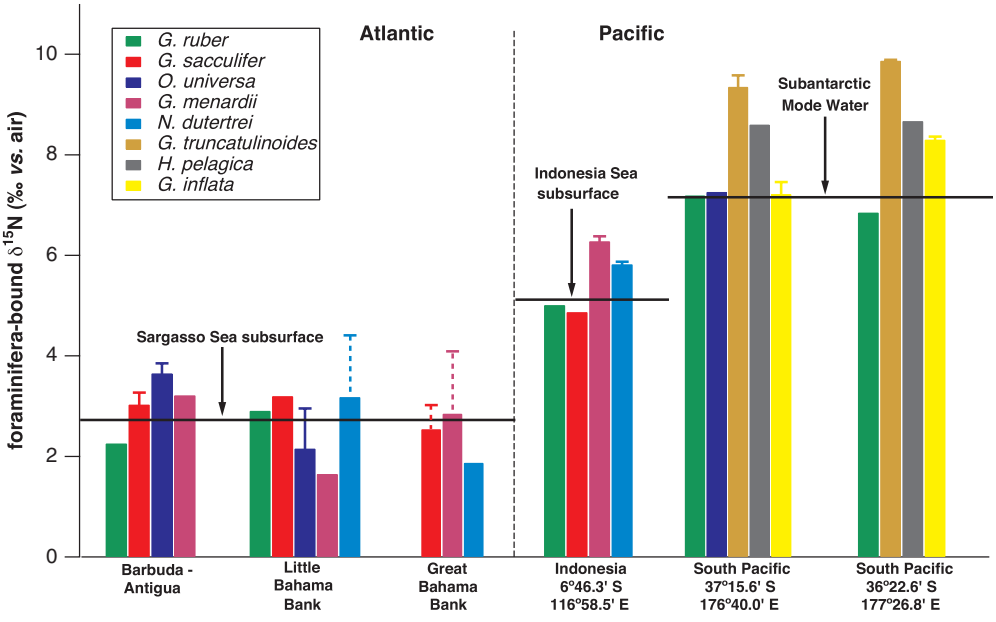

Fig. 1. Foraminifera-bound N $\delta^{15}N$ in surface sediment and core-top samples, compared with measured or estimated subeuphotic zone nitrate. Data are from the North Atlantic near Barbuda-Antigua (5 to 10 cm in gravity core EN18, >250-μm size fraction), Little Bahama Banks (grouped box cores, 0 to 5 cm, >500 μm), Great Bahama Banks (grouped box cores, 0 to 5 cm, from 75- to 125-μm as well as >500-μm size fractions), the Makassar-Bali Basin east of Indonesia (1 to 2 cm depth in multicore, >150 μm), and the western South Pacific near New Zealand (0 to 1 cm in multicores, >150 μm) (*23*). Here and in subsequent figures, solid error bars indicate SD for replication of the full foraminifera cleaning and analysis protocol; dashed error bars are for different surface sediment samplings in the same region. The three black horizontal lines indicate the estimated $\delta^{15}N$ of the subsurface nitrate supply in each of these regions (i.e., the nitrate directly below the euphotic zone): 200 m at the Bermuda Atlantic Time-series Study (BATS) site (*11*), 100 m in the Makassar-Bali Basin, and, in the case of the western South Pacific samples, Subantarctic Mode Water as measured in the Subantarctic Zone south of Australia (*40*), which forms nearby and should be relatively unaltered at this site.

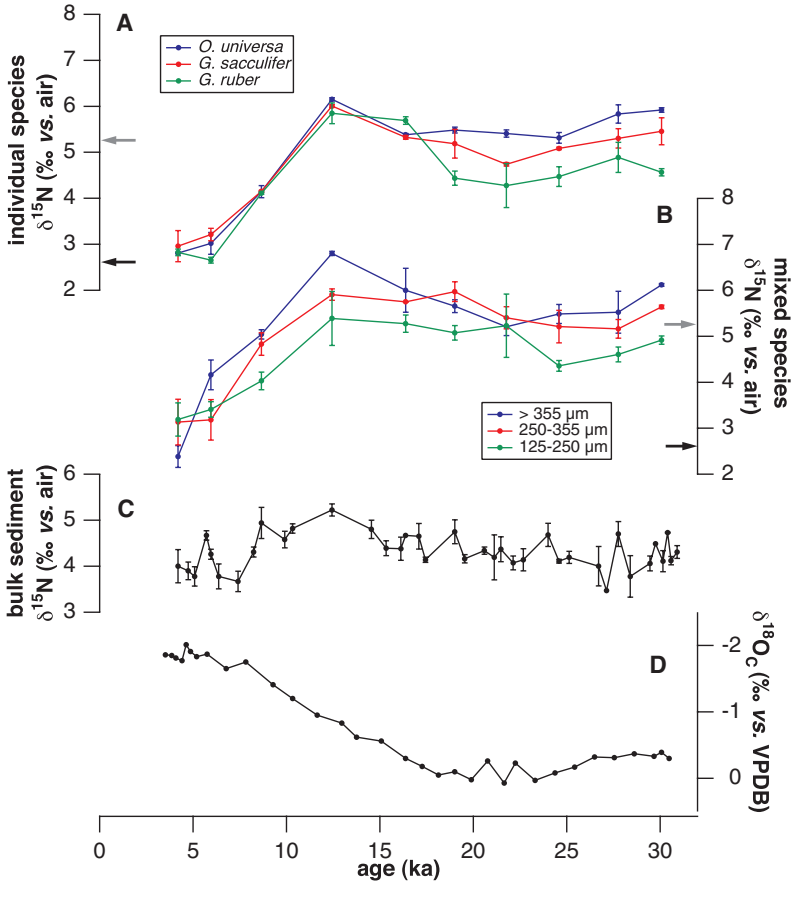

Fig. 2. Foraminifera-bound and bulk sedimentary $\delta^{15}N$ in the Caribbean Sea from ODP 999A (12°45´N, 78°44´W; 2827 m; sedimentation rate ~4 cm per 1000 years) during the past 30,000 years (ka, thousands of years ago). (**A**) Planktonic foraminifera-bound $\delta^{15}N$ of individual species. Blue, *O. universa*; red, *G. sacculifer*; green, *G. ruber*. *O. universa* and *G. sacculifer* were picked from the >355-μm size fraction; *G. ruber* was picked from the >250-μm size fraction. (**B**) Planktonic foraminifera-bound $\delta^{15}N$ of different foraminifera size fractions. Blue, >355 μm; red, 250 to 355 μm; green, 125 to 250 μm. *Neogloboquadrina dutertrei*, *O. universa*, *G. sacculifer*, and *G. ruber* are abundant in the >355-μm size fraction. *O. universa*, *G. sacculifer*, and *G. ruber* are abundant in the 250- to 355-μm size fraction. *G. ruber* and *G. bulloides* are abundant in the 125- to 250-μm size fraction. Black and gray arrows indicate present-day subeuphotic zone and subthermocline nitrate $\delta^{15}N$ in the western North Atlantic, respectively (*12*). (**C**) Bulk sedimentary $\delta^{15}N$, with error bars indicating SD calculated from replicates. (**D**) $\delta^{18}O$ of *G. ruber* (pink) calcite [‰ versus Vienna Pee Dee belemnite (VPDB) standard] from (*41*). The age model is from (*41*), based on ^{14}C dating and $\delta^{18}O$ correlation.

open ocean where N fixation is thought to be focused, seafloor processing increases the $\delta^{15}N$ of bulk sedimentary N from that of sinking N (*13*), reducing confidence in sedimentary N as a recorder of sinking-flux $\delta^{15}N$. In these environments, where little marine organic N is preserved and buried, foreign (e.g., terrestrial) N can also contaminate the regional ocean signal.

In the subtropical and tropical ocean, planktonic foraminifera are an important component of the sinking flux to the sediments. The organic matrix laid down in foraminiferal tests is physically protected by the test during sedimentary diagenesis (*14*, *15*). Thus, foraminifera-bound N is a promising paleoceanographic archive in sites where sedimentary processes may complicate bulk sediment N isotope records (*16*, *17*). Planktonic foraminifera are heterotrophic zooplankton, and many species also have dinoflagellate symbionts. They obtain N mostly from particulate organic matter (POM), including phyto- and zooplankton (*18*). The $\delta^{15}N$ of zooplankton, including foraminifera, tends to be ~3‰ higher than that of their food source because of preferential excretion of ^{14}N-rich ammonia (*19*, *20*). The ammonia excretion, in turn, lowers the $\delta^{15}N$ of POM relative to the N supply to the euphotic zone (*21*). In the modern Sargasso Sea, the $\delta^{15}N$ of subsurface nitrate supplied to the euphotic zone is 2 to 3‰ (*11*), the $\delta^{15}N$ of suspended POM is closer to 0‰ (*21*, *22*), and the $\delta^{15}N$ of zooplankton appears to center around 2 to 3‰ (*21*), similar to the $\delta^{15}N$ of nitrate supply and the N export (*22*). Thus, we expect the $\delta^{15}N$ of foraminifera to be similar to and correlated with the integrated $\delta^{15}N$ of the new N supply to the euphotic zone, including nitrate from below and N fixation.

We measured the foraminifera-bound $\delta^{15}N$ in surface sediments from several regions (*23*) (fig. S3) and compared them with the $\delta^{15}N$ of subsurface nitrate. The foraminifera-bound $\delta^{15}N$ of most species from these locations is close to (rarely more than 1‰ different from) the $\delta^{15}N$ of the shallow thermocline nitrate available for upward transport into the euphotic zone (Fig. 1). At some sites, deeper-dwelling species (in particular, *Globorotalia truncatulinoides* in the southwest Pacific samples) have a higher $\delta^{15}N$ than other species, which is best explained by the broadly observed increase in POM $\delta^{15}N$ with depth below the euphotic zone (*24*). One weakness of the comparison in Fig. 1 is that it does not take into account N fixation as a low-$\delta^{15}N$ N source within the euphotic zone that augments the nitrate supply, but this simplification appears reasonable (*23*).

Foraminifera-bound $\delta^{15}N$ and bulk sedimentary $\delta^{15}N$ were measured in sediments representing the past 30,000 years at Ocean Drilling Program (ODP) Site 999A in the Columbian Basin of the Caribbean Sea. In individual foraminifera species (Fig. 2A) as well as in mixed foraminifera samples of varying sizes (Fig. 2B), the LGM $\delta^{15}N$ is higher than the interglacial values. Focusing on the picked species data, the interglacial $\delta^{15}N$ is 2.7 to 3.2‰, similar to the thermocline nitrate $\delta^{15}N$ observed today in the tropical and subtropical western North Atlantic (*11*, *12*). The glacial $\delta^{15}N$ is 4.3 to 5.9‰, varying with species. This is generally close to the $\delta^{15}N$ of modern deep Atlantic nitrate measured just below the thermocline, 5.0 to 5.5‰ (*11*, *12*). The higher foraminifera-bound $\delta^{15}N$ in the LGM could be due to higher mean ocean nitrate $\delta^{15}N$ at that time. However, in relevant (i.e., nonpolar) open-ocean records, which derive from various oceanographic environments, there is as yet no evidence for a 2‰ decrease in mean ocean nitrate $\delta^{15}N$ upon deglaciation (*25*).

The low $\delta^{15}N$ of Holocene and surface sediment foraminifera from the North Atlantic tracks the low $\delta^{15}N$ of thermocline nitrate in the region, which in turn derives from the remineralization of newly fixed N. Thus, we interpret the high LGM foraminiferal $\delta^{15}N$ to reflect a weakening in the $\delta^{15}N$ decrease that occurs upward through the thermocline in the modern North Atlantic, such that the euphotic zone was supplied with nitrate with a $\delta^{15}N$ much more similar to the nitrate currently found at the base of the thermocline (Fig. 3). This most likely requires that N fixation was much reduced in the ice age Atlantic; a simple estimation, assuming no glacial-to-interglacial changes in thermocline circulation, suggests that it was ~20% of the Holocene rate (*23*) (fig. S5).

In addition to the clear glacial-to-interglacial change, there is a small (0.5 to 1.5‰) deglacial maximum in $\delta^{15}N$ apparent in each of the individual species records and in at least the >355-μm size fraction record. This feature, which is common in the deglacial section of sediment records from all basins (*25*), most likely reflects a peak in the $\delta^{15}N$ of mean ocean nitrate. It may result from a transient deglacial peak in water column denitrification relative to sediment denitrification and/or from a transient N loss from the ocean (*16*), the former process better matching the available data (*26*). Our record at Site 999 suggests that the deglacial $\delta^{15}N$ maximum is relatively weak in comparison to observations from denitrification-influenced records, but we

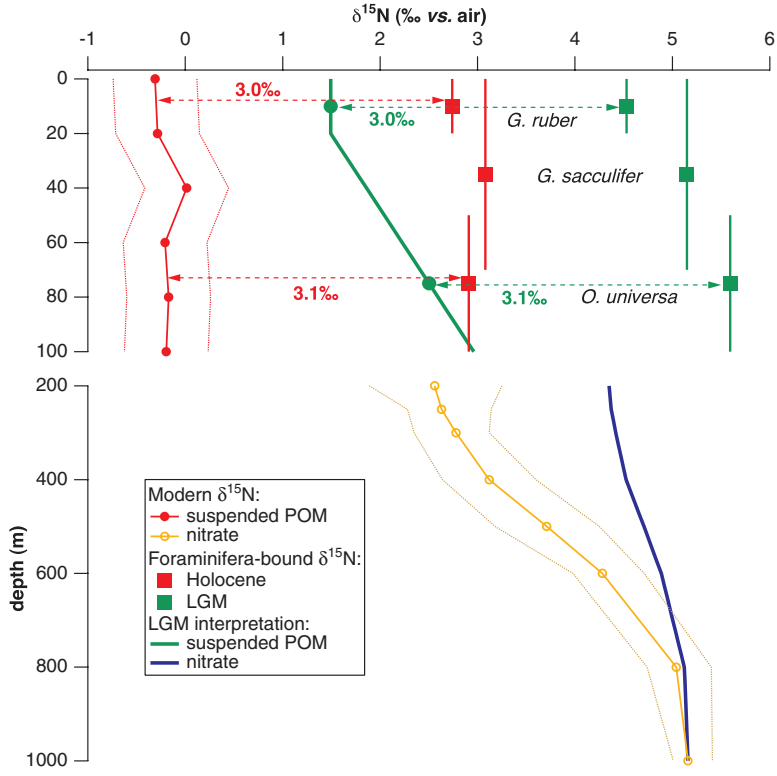

Fig. 3. Depth profile of $\delta^{15}N$ of suspended POM and nitrate in western North Atlantic during the present interglacial and the last ice age. Solid red circles denote the $\delta^{15}N$ of suspended particles in the surface 100 m near the Bermuda Atlantic Time-series Site (BATS) averaged over 1985 to 1988 [data from (*31*)]; dotted lines indicate 1 SD. Note that the suspended POM $\delta^{15}N$ increase accompanying the decreasing POM concentration below the euphotic zone (*24*), mentioned in the text, occurs below the depth range shown here. Orange circles denote average $\delta^{15}N$ of nitrate in the upper 200 to 1000 m at BATS (*11*); dotted lines indicate the measured range. Solid red and green squares denote foraminifera-bound $\delta^{15}N$ during the Holocene and the LGM, respectively. Foraminiferal depth maxima are taken from (*30*). Green and blue lines are proposed LGM depth profiles of the $\delta^{15}N$ of suspended POM in the photic zone and of nitrate in the thermocline (POM calculated from LGM-to-Holocene changes, using the depth ranges indicated for *G. ruber* and *O. universa* and assuming a constant foraminifera-POM $\delta^{15}N$ relationship for each of these two species; nitrate calculated from the *G. ruber* change).

suspect that it was overprinted by an increase in Atlantic N fixation at that time (Fig. 4, dashed interval).

The Caribbean foraminiferal $\delta^{15}N$ record is similar to the bulk sediment $\delta^{15}N$ record from Cariaco Basin (*27*, *28*) (Fig. 4). The Cariaco Basin record is from anoxic waters, and seafloor isotopic alteration and allochthonous N are demonstrably unimportant there today (*29*). However, the basin's barriers to circulation have complicated the interpretation of its $\delta^{15}N$ record, potentially affecting its changes. Nonetheless, the published interpretation of the deglacial $\delta^{15}N$ decrease in the Cariaco record—enhanced Atlantic N fixation upon deglaciation (*27*, *28*)—is supported by our open Caribbean foraminiferal data.

The foraminiferal species *Orbulina universa*, *Globigerinoides sacculifer*, and *Globigerinoides ruber* have similar $\delta^{15}N$ during the deglaciation and interglacial; however, they are coherently different during the LGM, with *O. universa* the highest and *G. ruber* the lowest (Fig. 2A). In the modern ocean, *G. ruber* is most abundant in the mixed layer, roughly the upper 30 m in this region. *G. sacculifer* inhabits a broader depth interval down to the deep chlorophyll maximum (DCM), at ~80 m in this region, and *O. universa* tends to have its abundance maximum near the DCM (*30*) (Fig. 3). Thus, the order of decreasing $\delta^{15}N$ during the last ice age coincides with habitats of progressively shallower depth.

In the modern tropical and subtropical western Atlantic, across the ~100-m-deep euphotic zone, suspended POM $\delta^{15}N$ is uniformly low relative to the thermocline nitrate supply, as a result of some combination of N fixation and N recycling (Fig. 3) (*21*, *22*). This rough uniformity is consistent with the similarity in $\delta^{15}N$ of *O. universa*, *G. sacculifer*, and *G. ruber*. The $\delta^{15}N$ divergence of these species during the last ice age probably arose from an increase with depth in euphotic zone suspended POM $\delta^{15}N$. This might have been the result of a larger $\delta^{15}N$ difference between N fixation and the subsurface nitrate supply, which, according to our data, had a higher $\delta^{15}N$ during the LGM. However, the species converge in $\delta^{15}N$ during the deglaciation, before the $\delta^{15}N$ of the nitrate supply had decreased, which suggests that this is not the sole explanation for the interspecific differences during the LGM.

In the modern Sargasso Sea, preferential ^{14}N recycling should work to lower the $\delta^{15}N$ of the mixed layer relative to the deeper euphotic zone (*31*), but this gradient is apparently diluted by N inputs to the entire euphotic zone, including N fixation. With less N fixation during the LGM, the recycling-driven $\delta^{15}N$ gradient may have been unobscured and thus stronger, leading to the clear $\delta^{15}N$ differences among species. It is also possible that, with less N fixation, the remaining fixation and its isotopic signal [as well as that of atmospheric deposition (*32*)] was focused in the warm, nutrient-poor surface mixed layer, isolated from the nitrate supply from below. In this scenario, the species' convergence in $\delta^{15}N$ at the $\delta^{15}N$ maximum marks the deglacial acceleration in Atlantic N fixation (Fig. 4).

Our bulk sediment $\delta^{15}N$ record from ODP Site 999 has limited correspondence to our foraminiferal records, possibly showing a deglacial maximum but only a weak (<0.5‰) glacial-to-interglacial decrease that is insignificant in a Student *t* test (Fig. 2C). We suspect that changing inputs of shelf material to Site 999 have altered the relationship of sinking to sedimentary N across the deglaciation. At Site 999, Holocene sediment has ~35% terrigenous material by weight, with ~60% during the LGM (*33*). Associated with this change, the $\delta^{13}C$ of organic matter is ~1‰ lower during the LGM (fig. S6), whereas marine POM $\delta^{13}C$ should have been higher (*34*). This is consistent with a greater proportion of terrestrial organic matter during the LGM. The sediment organic carbon–total nitrogen ratio is lower in the LGM interval (fig. S6), and distinct trends in this ratio during the LGM and Holocene intervals imply a greater contribution of clay-bound N during the LGM (fig. S7). Both terrestrial organic matter and clay-bound N tend to be low in $\delta^{15}N$ (*35*) and would have worked to lower bulk sediment $\delta^{15}N$ during the last ice age, and thus would have destructively interfered with the oceanic change apparent in the foraminiferal $\delta^{15}N$ data.

The Site 999 data indicate that N fixation in the Atlantic was low during the LGM, when water column denitrification in the eastern Pacific and Arabian Sea was reduced (Fig. 4) and when sedimentary denitrification was probably also much lower (*36*). In this context, the LGM-to-Holocene increase in N fixation is consistent with a proposed negative feedback on ocean N content, due to N fixation: Denitrification-driven deficits in N relative to phosphorus (P) stimulate N fixation because N fixers are favored in N-depleted, P-bearing surface waters (*37*), causing N fixers to restore the ocean N:P ratio toward the ~16:1 "Redfield" ratio of plankton (*38*, *39*).

It has been argued that the micronutrient iron controls or modulates N fixation rate (*3*, *4*). The higher dust flux during the last ice age has been proposed to have caused higher N fixation at that time (*3*, *4*), a hypothesis apparently disproved by

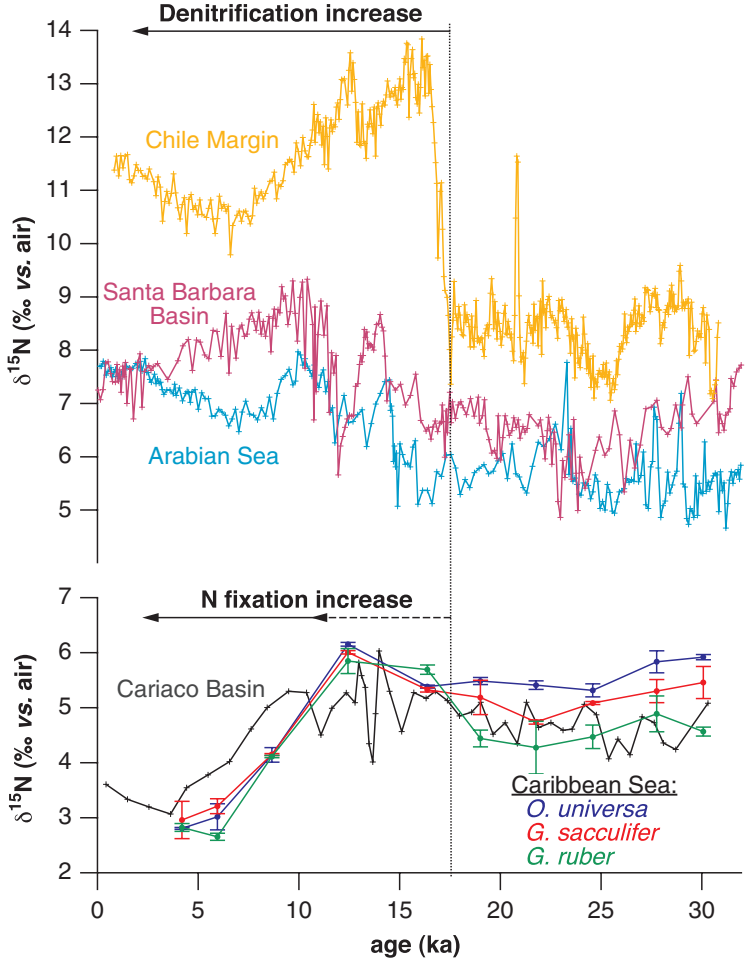

Fig. 4. Comparison of the ODP 999 species-specific foraminifera-bound $\delta^{15}N$ records for the past 30,000 years with bulk sediment $\delta^{15}N$ records from each of the major water column denitrification zones and from the nearby Cariaco Basin (*27*). Denitrification zone records are from the eastern Pacific off Chile (*42*), the eastern Pacific off California (Santa Barbara Basin) (*43*), and the Arabian Sea off Oman (*44*) (fig. S3).

our data for the Atlantic. However, we have not constrained the history of N fixation in the Indo-Pacific, where iron is typically more scarce. Moreover, although our results demonstrate a response from N fixation that works to stabilize the N budget, they do not preclude a glacial-to-interglacial decrease in the N inventory. Reconstruction of N fixation in the other basins and better information about the timing of changes should help to quantify the strength of the N fixation feedback and the limits that it places on the ocean N inventory. Foraminifera-bound N will facilitate this effort.

References and Notes

1. M. A. Altabet, R. Francois, D. W. Murray, W. L. Prell, *Nature* **373**, 506 (1995).
2. R. S. Ganeshram, T. F. Pedersen, S. E. Calvert, D. W. Murray, *Nature* **376**, 755 (1995).
3. P. G. Falkowski, *Nature* **387**, 272 (1997).
4. W. S. Broecker, G. M. Henderson, *Paleoceanography* **13**, 352 (1998).
5. M. B. McElroy, *Nature* **302**, 328 (1983).
6. E. Wada, A. Hattori, *Geochim. Cosmochim. Acta* **40**, 249 (1976).
7. $\delta^{15}N = \{[(^{15}N/^{14}N_{sample})/(^{15}N/^{14}N_{reference})] - 1\} \times 1000‰$, where the reference is N_2 in air.
8. J. A. Brandes, A. H. Devol, *Geochim. Cosmochim. Acta* **61**, 1793 (1997).
9. C. C. Barford, J. P. Montoya, M. A. Altabet, R. Mitchell, *Appl. Environ. Microbiol.* **65**, 989 (1999).
10. D. Karl *et al.*, *Biogeochemistry* **57–58**, 47 (2002).
11. A. N. Knapp, D. M. Sigman, F. Lipschultz, *Global Biogeochem. Cycles* **19**, GB1018 (2005).
12. A. N. Knapp, P. J. DiFiore, C. Deutsch, D. M. Sigman, F. Lipschultz, *Global Biogeochem. Cycles* **22**, GB3014 (2008).
13. M. A. Altabet, R. Francois, *Global Biogeochem. Cycles* **8**, 103 (1994).
14. K. King Jr., P. E. Hare, *Micropaleontology* **18**, 285 (1972).
15. L. L. Robbins, K. Brew, *Geochim. Cosmochim. Acta* **54**, 2285 (1990).
16. M. A. Altabet, W. B. Curry, *Global Biogeochem. Cycles* **3**, 107 (1989).
17. T. Nakatsuka *et al.*, *Geophys. Res. Lett.* **22**, 2525 (1995).
18. M. E. Uhle *et al.*, *Limnol. Oceanogr.* **44**, 1968 (1990).
19. D. M. Checkley Jr., C. A. Miller, *Deep Sea Res. I* **36**, 1449 (1989).
20. M. E. Uhle, S. A. Macko, H. J. Spero, M. H. Engel, D. W. Lea, *Org. Geochem.* **27**, 103 (1997).
21. J. P. Montoya, E. J. Carpenter, D. G. Capone, *Limnol. Oceanogr.* **47**, 1617 (2002).
22. M. A. Altabet, *Deep Sea Res.* **35**, 535 (1988).
23. See supporting material on *Science* Online.
24. K. Mintenbeck, U. Jacob, R. Knust, W. E. Arntz, T. Brey, *Deep Sea Res. I* **54**, 1015 (2007).
25. S. J. Kao, K. K. Liu, S. C. Hsu, Y. P. Chang, M. H. Dai, *Atmos. Chem. Phys. Discuss.* **5**, 1017 (2008) and references therein.
26. C. Deutsch, D. M. Sigman, R. C. Thunell, A. N. Meckler, G. H. Haug, *Global Biogeochem. Cycles* **18**, GB4012 (2004).
27. G. H. Haug *et al.*, *Paleoceanography* **13**, 427 (1998).
28. A. N. Meckler *et al.*, *Global Biogeochem. Cycles* **21**, GB4019 (2007).
29. R. C. Thunell, D. M. Sigman, F. Muller-Karger, Y. Astor, R. Varela, *Global Biogeochem. Cycles* **18**, GB3001 (2004).
30. A. C. Ravelo, R. G. Fairbanks, *Paleoceanography* **7**, 815 (1992).
31. M. A. Altabet, *Limnol. Oceanogr.* **34**, 1185 (1989).
32. M. G. Hastings, D. M. Sigman, F. Lipschultz, *J. Geophys. Res.* **108**, 4790 (2003).
33. G. Mora, J. I. Martinez, *Paleoceanography* **20**, PA4013 (2005).
34. J. P. Jasper, J. M. Hayes, *Nature* **347**, 462 (1990).
35. R. E. Sweeney, I. R. Kaplan, *Mar. Chem.* **9**, 145 (1980).
36. J. P. Christensen, *Cont. Shelf Res.* **14**, 547 (1994).
37. D. W. Schindler, *Science* **195**, 260 (1977).
38. A. C. Redfield, *Am. Sci.* **46**, 205 (1958).
39. W. S. Broecker, *Prog. Oceanogr.* **11**, 151 (1982).
40. P. J. DiFiore *et al.*, *J. Geophys. Res.* **111**, C08016 (2006).
41. M. W. Schmidt, H. J. Spero, D. W. Lea, *Nature* **428**, 160 (2004).
42. R. De Pol-Holz *et al.*, *Geophys. Res. Lett.* **33**, L04704 (2006).
43. E. Emmer, R. C. Thunell, *Paleoceanography* **15**, 377 (2000).
44. M. A. Altabet, M. J. Higginson, D. W. Murray, *Nature* **415**, 159 (2002).

45. We thank J. Bernhard and D. McCorkle for supplying surface sediment samples; Y. Wang, M. Coray, and S. Bishop for technical assistance; B. Brunelle for advice; and two anonymous reviewers for comments. Supported by NSF grants ANT-0453680, OCE-9981479, and OCE-0447570 (D.M.S.), OCE-0220776, OCE-0341412, and OCE-0502504 (Y.R.), and OCE-0437366 and OCE-0350794 (J. Bernhard), a Schlanger Ocean Drilling Fellowship (H.R.), BP through the Princeton Carbon Mitigation Initiative, and Deutsche Forschungsgemeinschaft grants (G.H.H.). This research used samples provided by the ODP, which is sponsored by NSF and participating countries under the management of Joint Oceanographic Institutions.

Supporting Online Material

www.sciencemag.org/cgi/content/full/1165787/DC1
Materials and Methods
SOM Text
Figs. S1 to S7
Table S1
References

10 September 2008; accepted 25 November 2008
Published online 18 December 2008;
10.1126/science.1165787
Include this information when citing this paper.

Drosophila Stem Cells Share a Common Requirement for the Histone H2B Ubiquitin Protease Scrawny

Michael Buszczak,* Shelley Paterno, Allan C. Spradling†

Stem cells within diverse tissues share the need for a chromatin configuration that promotes self-renewal, yet few chromatin proteins are known to regulate multiple types of stem cells. We describe a *Drosophila* gene, *scrawny* (*scny*), encoding a ubiquitin-specific protease, which is required in germline, epithelial, and intestinal stem cells. Like its yeast relative UBP10, Scrawny deubiquitylates histone H2B and functions in gene silencing. Consistent with previous studies of this conserved pathway of chromatin regulation, *scny* mutant cells have elevated levels of ubiquitinylated H2B and trimethylated H3K4. Our findings suggest that inhibiting H2B ubiquitylation through *scny* represents a common mechanism within stem cells that is used to repress the premature expression of key differentiation genes, including Notch target genes.

Stem cells are maintained in an undifferentiated state by signals that they receive within the niche and are subsequently guided toward particular fates upon niche exit (*1*). Within embryonic stem (ES) cells and during differentiation, cell state changes are controlled at the level of chromatin by alterations involving higher-order nucleosome packaging and histone tail modifications (*2*). Polycomb group (PcG) and Trithorax group (trxG) genes influence key histone methylation events at the promoters of target genes, including H3K27 and H3K4 modifications associated with gene repression and activation, respectively, but few other genes with a specific role in stem cells are known.

Histone H2A and H2B monoubiquitylation play fundamental roles in chromatin regulation, and H2A ubiquitylation has been linked to PcG-mediated gene repression and stem cell maintenance. The mammalian Polycomb repressive complex 1 (PRC1) component RING1B is an H2A ubiquitin ligase that is required to block the elongation of poised RNA polymerase II on bivalent genes in ES cells (*3*). Mutations in the PRC1 component BMI-1, which complexes with RING1B, cause multiple types of adult stem cells to be prematurely lost (*4*). The role of H2B ubiquitylation in stem cells is unclear, however. In yeast, ubiquitylation of histone H2B by the RAD6 and BRE1 ligases controls H3K4 methylation (H3K4me3) (*5*, *6*), a process that requires the polymerase accessory factor PAF1 (*7*, *8*). Conversely, H2B deubiquitylation by the ubiquitin-specific protease (USP) family member UBP10 is required for silencing telomeres, ribosomal DNA, and other loci (*9*). The *Drosophila* homolog of BRE1, dBRE1, also is needed for H3K4 methylation, which suggests that this

Howard Hughes Medical Institute Research Laboratories, Department of Embryology, Carnegie Institution, Baltimore, MD 21218, USA.

*Present address: University of Texas Southwestern Medical Center, Department of Molecular Biology, Dallas, TX 75390, USA.

†To whom correspondence should be addressed. E-mail: spradling@ciwemb.edu